International Journal of Energy
ISSN: 2957-9473 | Vol. 2, No. 3, 2023

Experimental Study on the Evolution of Flame Trajectory Line Length for Two Buoyancy-controlled Linear Jet Flames at Different Inclined Angles

Le Chang *, Qiang Wang

School of Automotive and Transportation Engineering, Hefei University of Technology, Hefei 230009, China

Abstract: This paper presents an experimental study of the flame trajectory line length for a buoyancy-controlled dual linear jet flame at different inclined angles (0° ~ 90°). Two nozzles of the same size (80mm*1mm) were used for the experiments, propane was used as the fuel, the range of fuel exit velocity was 0.63 ~ 4.17m/s, the range of burner spacing was 0-0.6m, and a digital camera was used to record the flame morphology. In this paper, a critical spacing Dc is introduced to indicate the change of flame height, and a prediction model of Dc and fuel exit velocity Uf is established to divide the flame trajectory length with spacing into two stages, namely: when S<Dc, the flame trajectory length increases significantly with the decrease of nozzle spacing; when S>Dc, the flame trajectory length does not change significantly with the increase of spacing, and finally approaches to a single free flame trajectory length. When S>Dc, the flame trajectory length did not change significantly with the increase of burner spacing, and finally approached to a single free flame trajectory length, so the flame trajectory length showed a complex non-monotonic evolution. Based on the analysis of the air entrainment, two global models are developed to predict the trajectory lengths of the buoyancy-controlled dual-jet flame system in two states with different initial inclined angles. the model was applied to correlate all the data in this study as well as the data in previous studies.

Keywords: Inclined Angles; Two Buoyancy-controlled Linear Jet Flames; Critical Burner Spacing; Flame Trajectory Line Length.

1. Introduction

Natural gas transmission pipeline leaks occur frequently and seriously damage the safety of people's lives and property [1,2]. In general, a ruptured pipeline carrying gas at high pressure can be approximated as a linear turbulent diffusion jet fire based on its root fire shape and large gas ejection velocity. Jet fires are a fundamental scientific problem in the field of combustion and fire research. Previously, the jet flame characteristics have been studied extensively, for the flame height has also been considered as one of the most important parameters of fire, and the previous research mainly focused on the vertical upward jet flame, while the reality of the flame may occur at different angles as well as multiple places at the same time, thus the study of the behavior characteristics of the interaction of two linear jet flames with different inclination angles and their laws, for the prevention of jet flame fusion leading to It is important to study the behavior of two linear jet flames with different inclination angles and their laws to prevent the jet flames from fusion leading to greater losses.

Sugawa et al [3] conducted experiments with rectangular burners with aspect ratios of 1:20 and 1:40 placed parallel to each other at 30cm above the ground using propane as fuel, and proposed a dimensionless model of flame height including nozzle size and burner spacing, but the experimental data did not fit the model well. Thomas et al [4] conducted experiments using two rectangular burners (width to length ratio of 1:2) to investigate the effect of burner spacing on turbulent diffusion flame interactions and found that the ratio of the merging flame height to a single free flame is 6/5; Hu et al. [5] conducted a series of experiments with a burner size of 142.5 mm × 2 mm and proposed a correlation between the flame merging probability and the dimensionless burner spacing D/Z_{f0}, in addition, by analyzing the effect of burner spacing variation on the air entrainment in the flame, a dimensionless formula was proposed based on the newly defined dimensionless heat release rate, using the "effective" entrainment perimeter (P=L+2W+S+αL) as the characteristic length, and deriving the normalized flame merging height and the newly defined dimensionless heat release rate exponential relationship; Li et al [6] quantified the flame merging probability and flame merged height for different burner spacing and different combustion rates using two parallel linear burners with aspect ratios (100 mm × 4 mm and 200 mm × 2 mm). A new dimensionless heat release rate including aspect ratio (n=L/W) is proposed to determine the flame merging probability. And the effect of ground on flame air coiling is analyzed to develop two new segmental models for predicting the merging probability. And the effective entrainment perimeter R of a single burner is introduced as the characteristic length to derive the flame height model; He et al [7] considered the effect of different size nozzles on the flame height and predict the correlation coefficient model for the flame height of a double rectangular pool fire with different aspect ratios and distances; Wan et al. [8] theoretically analyzed the effect of air entrainment on two buoyant turbulent flames in open space and propose a flame height model related to the flame heat release rate; Ji et al. [9] conducted an experimental study on two jet flames with the same size and different heat release rates, and found that the interaction law and air entrainment mechanism are more complicated compared with two identical HRR flames, and proposed physical models for double rectangular flame heights and air entrainment applicable to different HRRs and the same HRR; Liu et al.[10]investigated the interaction of two parallel rectangular flames by a combination of experimental observation and theoretical analysis. It was found that for a given burner size parameter, the P_m data and

the dimensionless flame spacing S/Zc for different interaction states can be well-fitted by the Boltzmann function. Finally, the prediction model of dimensionless flame height Z_f/ D in different states is established by defining a new characteristic length for the two flames as a whole.

For the study of a single fire source, Tao et al [11] proposed the relationship between flame length and heat release rate at the initial angle through a series of experimental studies on three circular nozzles with different diameters, and found that the entrainment coefficient C_1 is linearly related to cosθ; an empirical model of flame length related to flame inclination angle, nozzle diameter and dimensionless heat release rate was proposed. Peters and Gore [12,13] studied the horizontal length of flame with initial angle in different Froude number states and proposed an analytical formula for the flame trajectory line. Wang [14] et al. conducted an experimental study on circular nozzles with initial inclination angle and established a model to estimate the horizontal extension length of a single jet flame with different diameters and inclination angle nozzles by correcting the dimensionless heat release rate; Zhang [15], Smith [16], Huang [17], Studer [18], Fang [19] and other researchers investigated the behavior and mechanism of horizontally oriented jet flames were studied, and a fitting model for the relevant flame length was proposed.

As can be seen from the above, previous studies have focused extensively on the behavior of dual jet flames in the common scenario of a free vertical jet or a single circular nozzle jet flame with an initial inclination angle and a horizontal jet. In contrast, the more common scenario in actual industrial processes, pipe leakage explosions and other diffusion combustion are multiple linear jet flames with different initial inclination angles. In the inclined state, the initial momentum of the fuel does not coincide with the flame buoyancy direction, and the air entrainmen will be more complex [20], so it is necessary to carry out a study of the behavioral characteristics and interactions of double diffusion jet flames under inclined conditions. In this paper, based on the previous work, we determine the quantitative relationship of the flame trajectory length of double flames under the coupling effect of different inclined angles and burner spacing through experimental observation and theoretical analysis, aiming to provide a reference basis for real industrial processes [21].

2. Experiment

The experimental setup is shown in Figure 1. Two identical linear burners made of 1 mm thick stainless steel were used, each burner consisted of a gas storage chamber and a linear nozzle, and the two linear nozzle outlets were kept at the same level for each experiment, with the gas storage chamber being 50 mm wide and 50 mm high, and the internal length L of the burner is 80 mm and the width W is 1 mm. The effective heat of combustion (ΔHc) was about 46.3 MJ/kg when the experiments were conducted with propane as the fuel and the HRR of the two burners was kept the same and controlled by two flow meters with the same accuracy (0.01 L/min), respectively [22]. The burner spacing S is the distance between the inner sides of the burner walls and ranges from 0 m ~ 0.6 m. In addition, experiments with a single linear nozzle at different angles were performed. The burner inclination angle θ was defined as the angle between the nozzle and the horizontal direction, varying from 0° to 90°, and the HRR of each burner ranged from 4.26 ~ 28.4 kW with an exit velocity of 0.63 ~ 4.17 m/s. Delichatsios [23] considered that the flame Froude number can determine whether the flame is controlled by buoyancy or momentum, when the flame Froude number $Fr_f = u_f \Big/ (\mathrm{g}d)^{1/2}(s+1)^{3/2}(\rho/\rho_\infty)^{1/4}(\overline{\Delta T_{f,\ a}}/T_\infty)^{1/2}$ is much less than 5, the flame is controlled by buoyancy, otherwise, it is controlled by momentum, and the Froude number calculated in this paper is 0.033935 ~ 0.2262 much less than 5, which means that the experiments are conducted under buoyancy control. In order to ensure the accuracy of the experiment, each experiment is repeated three times. The experimental working conditions are shown in Table 1

The flame images were recorded with a CCD camera (25 fps, 1920 × 1080 pixels). the CCD camera was positioned 2 m away from the centerline position of the two nozzles, and each experiment was filmed for 3~4 min after the flame stabilization. In this study, a more accurate and standard image processing method was used [24-26], as shown in Figure 2 for the flame processing process, for each experimental condition, 20s of stabilized flame video was first extracted and converted to 500 flame images, and the flame images were converted to gray images, and then the image processing method developed by Ostu [24] was used to The flame contours were post-processed and converted to binary images, and the probability contour of flame appearance was extracted from the binary images, and the average flame trajectory length was obtained by analyzing the probability contour of flame presence. The average flame trajectory length was determined as the trajectory length between the burner exit and the highest position with a flame interval probability of 0.5. This is shown in Figure 3.

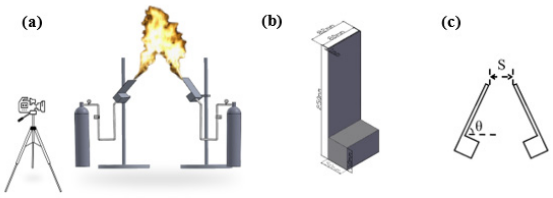


Figure 1. (a) Experimental setup; (b) nozzle size; (c) definition of burner inclination and spacing

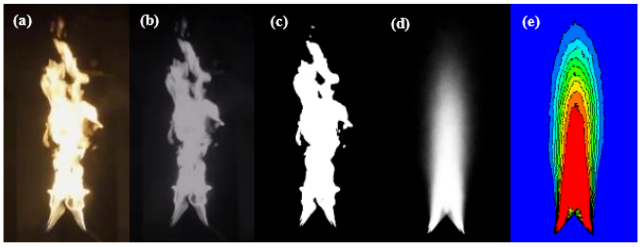


Figure 2. Flame processing method: (a) Original flame image, (b) Gray image, (c) Binary image, (d) Average image, (e) Flame contour

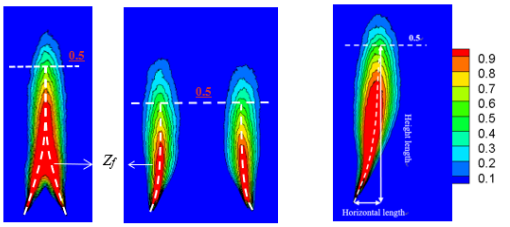


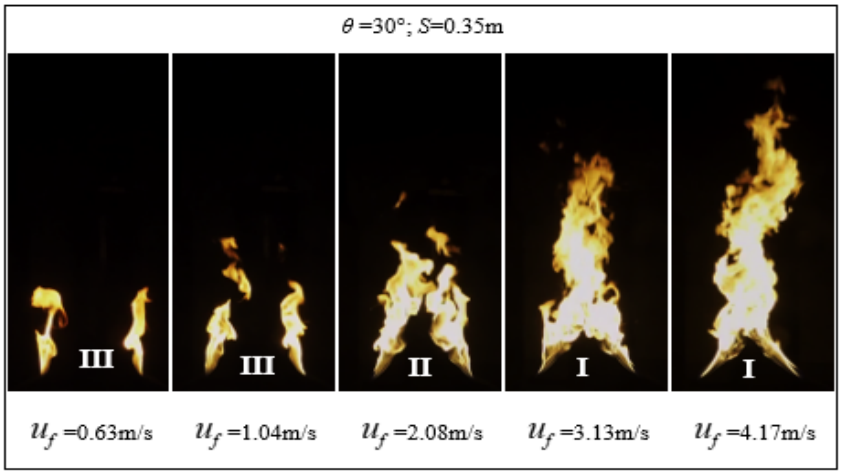
Figure 3. (a) and (b) are schematic diagrams of the definition of the trajectory lengths of the merged and unmerged flames, respectively, and (c) is the definition of the horizontal width and vertical height of a single flame

Table 1. Experimental conditions

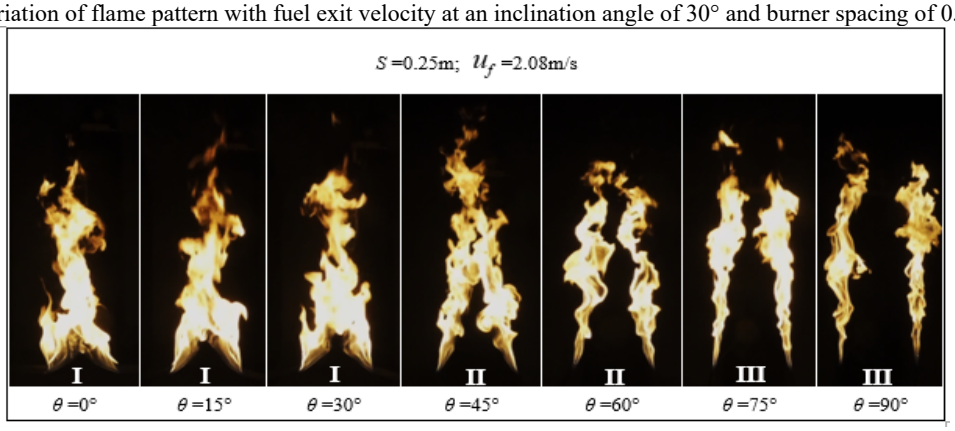
Test condition	Inclined Angle	Burners' spacing distance (m)	Fuel velocity (m/s)	HRR (kW)
Double fires	90°/75°/60°/45°/ 30°/15°/0°	0/0.025/0.05/0.075/0.1/0.15/0.2/0.25/0.3/ 0.35/0.4/0.45/0.5/0.6	0.63−4.17	4.26 -28.4
Single fire	90°/75°/60°/45°/ 30°/15°/0°	-	0.63−4.17	4.26 -28.4

3. Results and Discussion

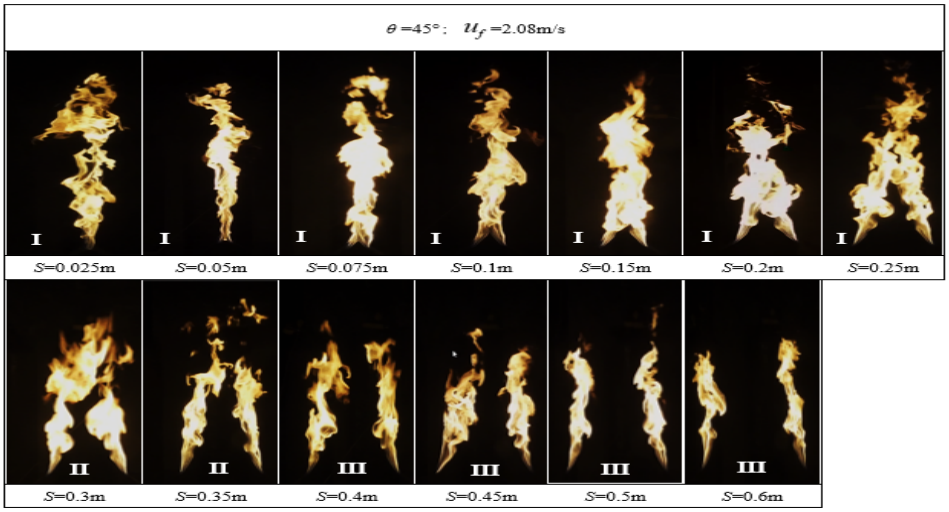
3.1. Combustion and Flame Merging State



a. Variation of flame pattern with fuel exit velocity at an inclination angle of 30° and burner spacing of 0.35m



b. Variaion of flame pattern with inclined angles at the burner spacing of 0.25m and the fuel exit velocity of 2.08m/s



c. Variation of flame pattern with burner spacing at the nozzle inclined angle of 45° and the fuel exit velocity of 2.08m / s

Figure 4. Typical images of flame interactions under different conditions

Figure 4 shows the change of flame state with flow rate, angle and spacing, and it can be observed that the flames show three fusion states, namely: (I) complete merging state; (II) intermittent merging state; (III) non-merging state; among them, Figure 4a shows that in the low flow rate state, the two flames are independent of each other (state III); with the increase of flow rate, the two flames inclined, and the flame has the tendency to be elongated (state II); with the further increase of the flow rate, the two flames are merged, and the flame height increases rapidly (state I); Figure 4b shows that, with the increase of the nozzle inclined angle, the flame gradually changes from the merging state (state I) to the independent free flame state (state III), and the flame height shows a complex non-monotonic change; in Figure 4c, it is shown that, under the fixed inclination angle and flow rate, with the increase of the distance between two flames, the flame gradually transforms from the completely merging state to the independent state, and finally approaches the single free, and the flame height changes show non-monotonicity.

3.2. Flame Trajectory Line Length

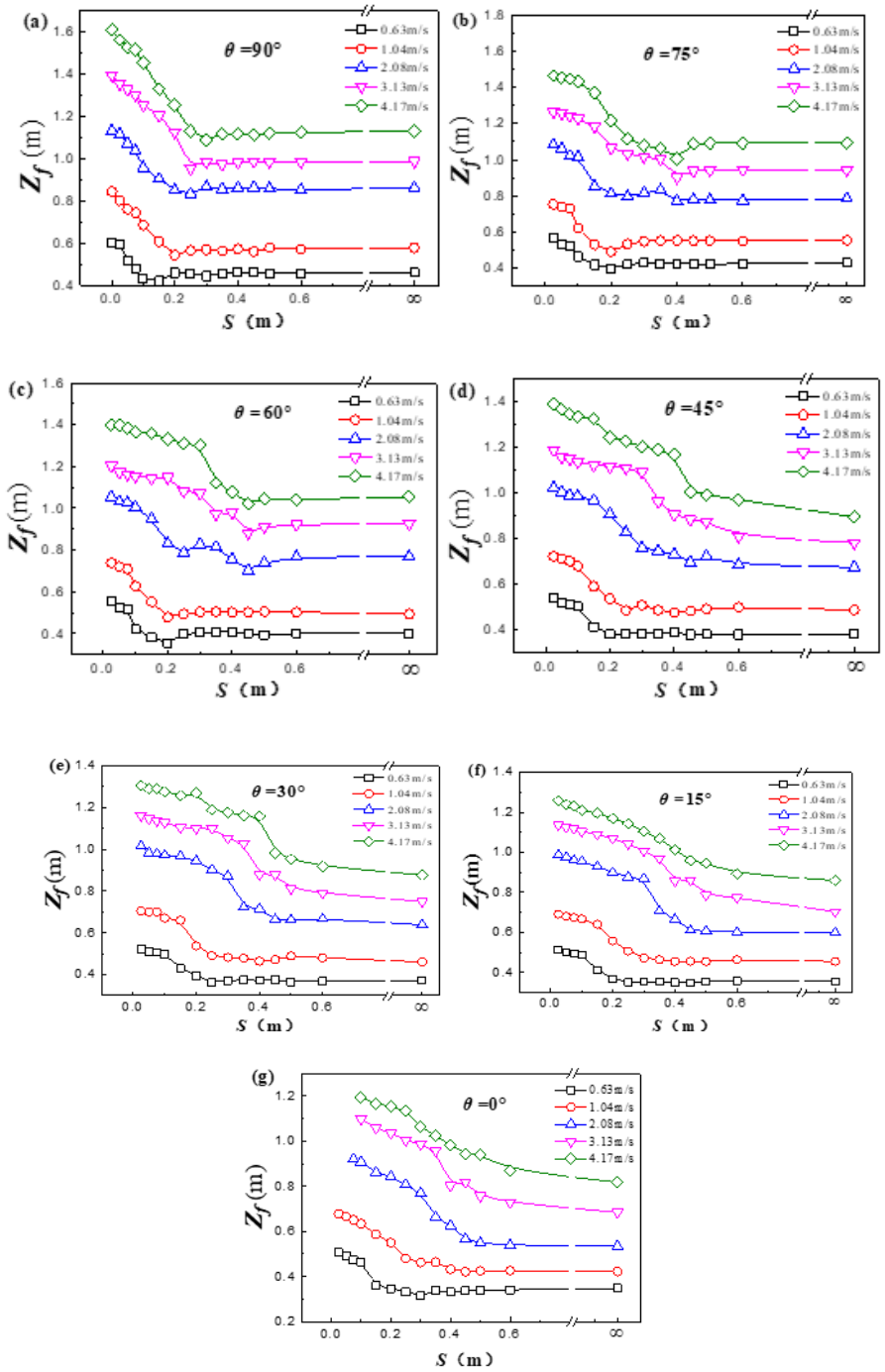


Figure 5. Flame trajectory length at different burner spacing for burner inclination angles from 0° to 90°

Figure 5 shows the experimentally obtained flame trajectory length variation at different burner spacing for burner inclination angles from 0° to 90°. It can be seen that at larger burner initial inclined angles (60°, 75°, 90°), the merging flame trajectory length gradually decreases with increasing burner spacing, and when a certain spacing is reached the flame trajectory length remains constant close to the individual free flame trajectory length, while at relatively small burner initial inclined angles, at larger experimental

conditions of flow rate (e.g. 45°, fuel flow rate of 3.13m/s and 4.17m/s), the flame trajectory line length decreases gradually with increasing burner spacing and does not reach equilibrium under the existing experimental conditions. Here, we define a critical spacing Dc for flame height variation, i.e., when the merged flame trajectory length decreases close to a single free flame trajectory length, the corresponding burner spacing is defined as the critical spacing for flame height variation at this time. The physical significance is that when the spacing does not exceed this critical value, the diffusion of unburned fuel dominates, resulting in an increase in the fusion flame trajectory length. For two flames with equal heat release rates, the pressure drop between the flames increases with increasing flame height at a defined initial nozzle inclined angle, and the greater the heat release rate, the stronger the restriction of air coiling; and for two flames with defined heat release rates, as the initial inclined angle of the burner increases, air enters between the two flames from the bottom and gradually increases the contact area with the inner flame surface, which in turn as the unburned fuel needs to travel a longer distance to burn completely, the merged flame height is more likely to change, i.e., the critical distance (Dc) of flame height change also increases with the increase of heat release rate and decreases with the increase of the initial inclined angle of the burner, as shown in Figure 6(a). In the "transition section" (stage II), the competition between the two mechanisms is dynamically balanced and the flame trajectory length changes weakly due to the limitation of air entrainment [10].

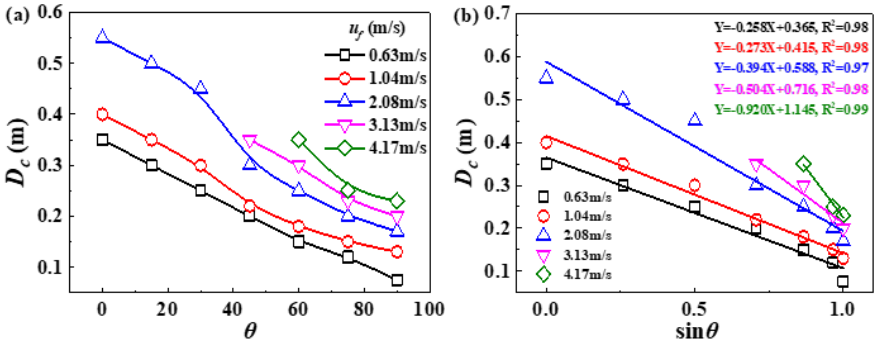


Figure 6. (a): Variation of Dc with θ; (b): Dc versus sinθ

Figure 6 shows the critical spacing Dc with $\sin\theta$ for different fuel exit velocities where the flame trajectory length changes, both showing a good linear relationship, which can be expressed as:

$$D_c = A_{u_f} \sin\theta + B_{u_f} \quad (1)$$

Where the fitted relationship between A_{u_f} and B_{u_f} for different flow rates u_f is shown in Figure 6(a), so then we have

$$A_{u_f} = -0.061u_f^2 + 0.114u_f - 0.32 \quad (2)$$

$$B_{u_f} = 0.049u_f^2 - 0.026u_f + 0.38 \quad (3)$$

Therefore, the critical spacing Dc can eventually be expressed as

$$D_c = \left(-0.061u_f^2 + 0.114u_f - 0.32\right)\sin\theta + 0.049u_f^2 - 0.026u_f + 0.38 \quad (4)$$

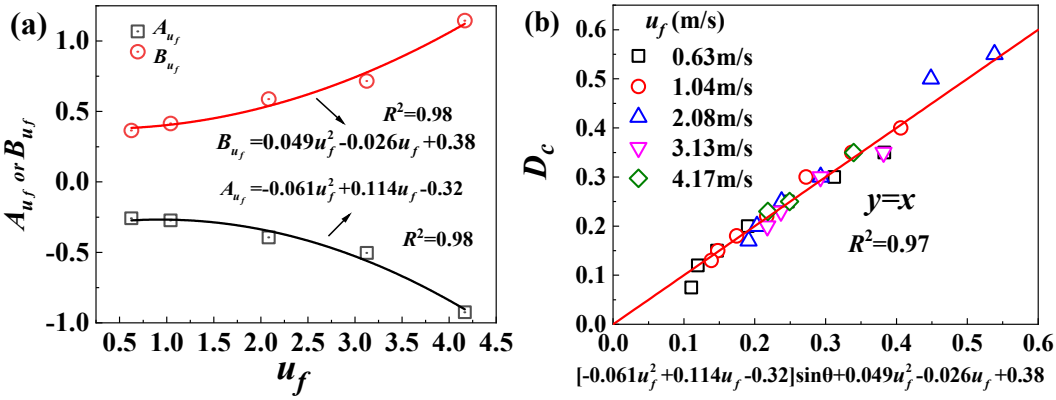


Figure 7. (a): Fitted parameters A_{u_f} and B_{u_f} versus u_f; (b): The relationship between Dc and u_f, sinθ

From the experiments and data can be inferred from the merging of flame trajectory line length and HRR, two nozzle spacing S, nozzle size (L, W) and nozzle inclined angle θ is closely related, so

$$Z_f = f(\dot{Q}, S, L, W, \theta) \quad (5)$$

For linear diffusion flames, the flame is thin and the flame tip is not easily identified. Therefore, it is necessary to consider the coiling perimeter of the flame. The two-flame system is symmetrical, and the coiling process of both flames can be considered as essentially the same. When S<Dc, it is reasonable to treat the merging flame as a zone flame. The heat release rate is the total fuel available for combustion of the flames, at which point the characteristic length of the array can be expressed as $P = L + 2W + 2d + S$; for a single flame i.e. when S>Dc, the characteristic length can be expressed as $P^* = L + W$. Specifically, the dimensionless flame trajectory length for different inclined angles can be expressed as

$$\frac{Z_{f,\theta}}{P} = A\left(\dot{Q}_P^*\right)^B \quad (6)$$

where when S<Dc, $\dot{Q}_P^*=\frac{2\dot{Q}}{T_\infty c_p \rho_\infty g^{1/2} P^{5/2}}$, when S>Dc, $\dot{Q}_{P^*}^*=\frac{\dot{Q}}{T_\infty c_p \rho_\infty g^{1/2} P^{*5/2}}$ [5],[6],[27],[28], were fitted to different angular data in two states, S<Dc and S>Dc, and it was found that the fitting index B varied around 0.48 for each angle, and the final average value of 0.48 was taken; the coefficient A has a good relationship with sinθ as shown in Figure 8, and its expressions are

$$A_1 = 0.446(\sin\theta)^3 - 0.159(\sin\theta)^2 + 0.198\sin\theta + 3.574 \quad (7)$$

$$A_2 = 0.565(\sin\theta)^3 - 0.244(\sin\theta)^2 + 0.767\sin\theta + 2.861 \quad (8)$$

The final equation for the length of the flame trajectory line is obtained as

$$\frac{Z_{f,\theta}}{P} = [0.446(\sin\theta)^3 - 0.159(\sin\theta)^2 + 0.198\sin\theta + 3.574]\dot{Q}_P^{*0.48}; S < D_c \quad (9)$$

$$\frac{Z_{f0,\ \theta}}{P^*} = [0.565(\sin\theta)^3 - 0.244(\sin\theta)^2 + 0.767\sin\theta + 2.861]\dot{Q}_{P^*}^{*0.48}; S > D_c \quad (10)$$

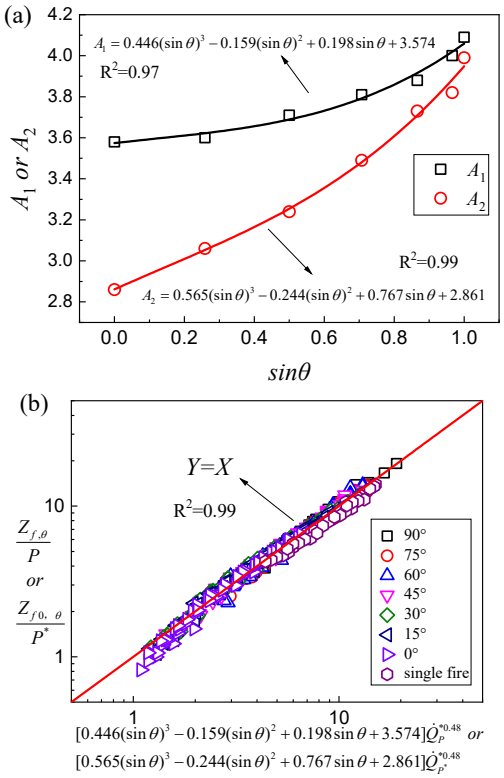


Figure 8. (a): Fitted coefficient A versus sinθ; (b): Dimensionless flame trajectory length model

When the burner spacing tends to infinity, the two flames at this point are in a completely independent state, and their combustion characteristics are identical to those of a single flame. As can be seen from Figure 5.6b, the model can predict the flame trajectory line length of a single linear fire source very well.

4. Conclusion

In this paper, the flame length scales of a two-flame system with two buoyant main turbulent diffusion linear jet flames coupled by burner spacing and angle are experimentally investigated. The merged flame trajectory line lengths are quantified The main findings are summarized as follows: (1) The flame pattern varies with the burner spacing, inclined angle and fuel exit velocity showing three states of fusion, i.e., fully merged, intermittently merged and non-merged; for a fixed inclined angle and fire source spacing, the flame height increases with the increase of fuel exit velocity; for a fixed fuel flow rate and fire source spacing, the flame height tends to decrease with the increase of inclined angle; for a fixed inclined angle and fuel exit velocity, the flame height shows a non-monotonic variation with the fire source spacing. (2) A critical spacing (Dc) is defined, and a prediction model of Dc and fuel exit velocity u_f is established to divide the state of flame trajectory line length with spacing into two stages namely: when S<Dc, the flame trajectory line length increases significantly with the decrease of nozzle spacing; when S>Dc, the flame trajectory line length does not change significantly with the increase of spacing and finally approaches to a single free flame trajectory line length, the complex non-monotonic evolution of the flame trajectory line length presented.(3) Based on the analysis of air coiled suction, the flame trajectory lengths in two states, S<Dc and S>Dc, are analyzed in terms of magnitudes, and by introducing new effective characteristic lengths, two global models are established to predict the trajectory lengths of the buoyancy-controlled bilinear jet flame system in two states with different initial inclined angles, respectively. The models are able to correlate well for all the data in this study.

Acknowledgments

This work was supported jointly by Fundamental Research Funds for the Central Universities of China (No. JZ2022HG PA0310).

References

[1] Wang Z, Zhou K, Zhang L, Nie X, Wu Y, Jiang J, et al. Flame extension area and temperature profile of horizontal jet fire impinging on a vertical plate. Process Safety and Environmental Protection 2021; 147:547–58. https://doi.org/ 10. 1016/j.psep.2020.11.028.

[2] Zhou K, Liu J, Jiang J. Prediction of radiant heat flux from horizontal propane jet fire. Applied Thermal Engineering 2016; 106:634–9. https:// doi.org/10. 1016/j. applthermaleng. 2016. 06. 063.

[3] Sugawa O, Takahashi W. Flame height behavior from multi-fire sources. Fire and Materials 1993; 17:111–7.

[4] Thomas PH. The size of flames from natural fires. Symposium (International) on Combustion 1963;9:844–59. https://doi.org/ 10.1016/ S0082-0784(63)80091-0.

[5] Hu L, Huang L, Wang Q, Kuwana K. Experimental study and analysis on the interaction between two slot-burner buoyant turbulent diffusion flames at various burner spacinges. Combustion and Flame 2017;186:105–13. https://doi.org/ 10.1016/ j.combustflame.2017.07.033.

[6] Li K, Ma Z, Huang X, Zou Y. Merging dynamics of dual parallel linear diffusion flames. Fire Safety Journal 2022; 127:103490. https://doi.org/10.1016/j.firesaf.2021.103490.

[7] He P, Wang P, Wang K, Liu X, Wang C, Tao C, et al. The evolution of flame height and air flow for double rectangular pool fires. Fuel 2019; 237:486–93. https://doi.org/ 10. 1016/j. fuel. 2018.10.027.

[8] Wan H, Ji J, Li K, Huang X, Sun J, Zhang Y. Effect of air entrainment on the height of buoyant turbulent diffusion flames for two fires in open space. Proceedings of the Combustion Institute 2017;36:3003–10. https://doi.org/ 10.1016/ j.proci. 2016.07.078.

[9] Ji J, Wan H, Gao Z, Fu Y, Sun J, Zhang Y, et al. Experimental study on flame merging behaviors from two pool fires along

the longitudinal centerline of model tunnel with natural ventilation. Combustion and Flame 2016; 173:307–18. https:// doi.org/ 10.1016/j.combustflame.2016.08.020.

[10] Liu N, Zhang S, Luo X, Lei J, Chen H, Xie X, et al. Interaction of two parallel rectangular fires. Proceedings of the Combustion Institute 2019;37:3833–41. https://doi. org/ 10. 1016/ j.proci.2018.06.158.

[11] Tao C, Shen Y, Zong R. Experimental determination of flame length of buoyancy-controlled turbulent jet diffusion flames from inclined nozzles. Applied Thermal Engineering 2016; 93:884–7. https:// doi.org/ 10.1016/j. applthermaleng. 2015. 09. 049.

[12] Peters N, Göttgens J. Scaling of buoyant turbulent jet diffusion flames. Combustion and Flame 1991;85:206–14. https://doi. org/ 10.1016/ 0010-2180(91)90188-H.

[13] Gore JP, Jian CQ. Analytical solution to the flame trajectory based on the analysis of "Scaling of buoyant turbulent jet diffusion flames" by N. Peters and J. Göttgens. Combustion and Flame 1993;93:336–7. https://doi.org/10.1016/0010-2180 (93) 90114-I.

[14] Wang Z, Jiang K, Zhao K, Guo P. Macroscopic characteristics and prediction model of horizontal extension length for syngas jet flame under inclined conditions. International Journal of Hydrogen Energy 2021;46:23091–9. https://doi. org/ 10. 1016/ j.ijhydene.2021.04.118.

[15] Zhang X, Hu L, Zhang X, Tang F, Jiang Y, Lin Y. Flame projection distance of horizontally oriented buoyant turbulent rectangular jet fires. Combustion and Flame 2017; 176:370–6. https:// doi.org/10.1016/j.combustflame.2016.10.016.

[16] Smith T, Periasamy C, Baird B, Gollahalli SR. Trajectory and Characteristics of Buoyancy and Momentum Dominated Horizontal Jet Flames From Circular and Elliptic Burners. Journal of Energy Resources Technology-Transactions of The Asme 2006;128:300–10.

[17] Huang Y, Li Y, Dong B. Radiant Heat Flux Profile of Horizontally Oriented Rectangular Source Fuel Jet Fires. Ind Eng Chem Res 2018; 57:1078–88. https://doi. org/ 10.1021/ acs.iecr. 7b03977.

[18] Studer E, Jamois D, Jallais S, Leroy G, Hebrard J, Blanchetière V. Properties of large-scale methane/hydrogen jet fires. International Journal of Hydrogen Energy 2009; 34:9611–9.

[19] Fang X, Zhang X, Hu L. Transitional behavior of vertical flame height of horizontally-oriented rectangular-source jet fires n.d.:8.

[20] Wang Q, Yan J, Wang B, Chang L, Palacios A. Experimental study on trajectory flame length and axial temperature distribution of inclined turbulent jet flames. Fire Safety Journal 2022;131:103623. https:// doi.org/ 10. 1016/ j.firesaf. 2022. 103623.

[21] Shan K, Shuai J, Yang G, Meng W, Wang C, Zhou J, et al. Numerical study on the impact distance of a jet fire following the rupture of a natural gas pipeline. International Journal of Pressure Vessels and Piping 2020; 187:104159. https:// doi. org/ 10.1016/j.ijpvp.2020.104159.

[22] Cetegen BM, Ahmed TA. Experiments on the periodic instability of buoyant plumes and pool fires. Combustion and Flame 1993; 93:157–84. https://doi.org/10.1016/0010-2180(93) 90090-P.

[23] Delichatsios MA. Transition from momentum to buoyancy-controlled turbulent jet diffusion flames and flame height relationships. Combustion and Flame 1993; 92:349–64. https:// doi.org/10.1016/0010-2180(93)90148-V.

[24] Otsu N. A Threshold Selection Method from Gray-Level Histograms. IEEE Trans Syst, Man, Cybern 1979;9:62–6. https:// doi.org/10.1109/TSMC.1979.4310076.

[25] Audouin L, Kolb G, Torero JL, Most JM. Average centreline temperatures of a buoyant pool fire obtained by image processing of video recordings. Fire Safety Journal 1995; 24:167–87. https://doi.org/10.1016/0379-7112(95)00021-K.

[26] Tang F, Hu LH, Delichatsios MA, Lu KH, Zhu W. Experimental study on flame height and temperature profile of buoyant window spill plume from an under-ventilated compartment fire. International Journal of Heat and Mass Transfer 2012; 55:93–101. https:// doi. org/ 10. 1016/j. ijheatmasstransfer. 2011.08.045.

[27] Huang Y, Wan H, Ding L, Ji J, Wang C. Research on the interaction between two line jet fires with unequal heat release rate at different burner distances. Fuel 2019; 258:116016. https:// doi.org/10.1016/j.fuel.2019.116016.

[28] Ji J, Wan H, Gao Z, Fu Y, Sun J, Zhang Y, et al. Experimental study on flame merging behaviors from two pool fires along the longitudinal centerline of model tunnel with natural ventilation. Combustion and Flame 2016; 173:307–18. https:// doi.org/ 10.1016/j.combustflame.2016.08.020.

[29] Palacios A, Rengel B, Wang Q, Hu L. Analysis of experimental flame shapes and blowout velocities of partially-premixed methane-air jet flames. Fuel 2020;269:117430. https://doi.org/ 10.1016/ j.fuel.2020.117430.